Function of Myosin-V in Filopodial Extension of Neuronal Growth Cones

Feng-Song Wang, Joseph S. Wolenski, Richard E. Cheney,* Mark S. Mooseker, Daniel G. Jay†

The molecular mechanisms underlying directed motility of growth cones have not been determined. The role of myosin-V, an unconventional myosin, in growth cone dynamics was examined by chromophore-assisted laser inactivation (CALI). CALI of purified chick brain myosin-V absorbed onto nitrocellulose-coated cover slips inhibited the ability of myosin-V to translocate actin filaments. CALI of myosin-V in growth cones of chick dorsal root ganglion neurons resulted in rapid filopodial retraction. The rate of filopodial extension was significantly decreased, whereas the rate of filopodial retraction was not affected, which suggests a specific role for myosin-V in filopodial extension.

A fundamental challenge in biology is to understand how cells move, particularly in regard to the formation of the nervous system as neurons establish precise synaptic connections with their targets over long distances. The motile tips of elongating axons and dendrites, neuronal growth cones, are responsible for the navigation, elongation, and maintenance of growing neurites (*1*). The dynamic filopodia of the growth cones play key roles in signal detection, motile force generation, and axon guidance (*2*). Actin polymerization is required for filopodial motility (*3*). Myosins, a diverse superfamily of actin-based mechanoenzymes, have also been suggested to function in filopodial motility (*2*, *4*–*6*), but evidence for the role of any particular myosin has been lacking. This is due to the existence of a large number of myosin isoforms in cells and the lack of specific pharmacological probes (*7*). To address whether a particular myosin functions in filopodial motility, we selectively inhibited myosin-V in chick dorsal root ganglion (DRG) neuronal growth cones. Chick brain myosin-V is a two-headed unconventional myosin with Ca^{2+}-calmodulin–sensitive enzymatic and mechanochemical activities and is present at the tips of dendritic and axonal processes (*8*, *9*).

To investigate the role of myosin-V in DRG neuronal growth cone motility, we used a procedure called chromophore-assisted laser inactivation (CALI), in which malachite green (MG) dye is covalently conjugated to an antibody. When the conjugated antibody is irradiated with pulses of laser light, the dye releases protein-damaging hydroxyl free radicals, resulting in inactivation of the bound antigen with minimal damage of or cross-linking to neighboring proteins (*10*–*11*). CALI has been shown to result in a simple loss of function similar to genetic loss of function (*12*). Microscale-CALI (micro-CALI), in which microscope optics are used to focus the laser beam onto a spot 10 μm in diameter, allows one to selectively irradiate a defined region of a growth cone while the unirradiated region serves as an internal control (*11*). Micro-CALI is useful for elucidating the in vivo function of a particular protein provided that MG-labeled antibody introduced into the cells binds to the native antigen and has no effect on the antigen activity without irradiation. To address the possible function of myosin-V, we used a polyclonal antibody to myosin-V (anti–myosin-V) that specifically recognizes epitopes in the COOH-terminal tail of the myosin-V heavy chain (*9*) and does not interfere with the mechanochemical and actin-binding properties associated with the NH_2-terminal globular head (*13*).

Myosin-V was present in all regions of cultured chick DRG neurons, was concentrated in the cell body and growth cone (Fig. 1A) (*9*, *14*), and overlapped with F-actin in filopodia (Fig. 1C). Microinjected MG-labeled anti–myosin-V (MG–anti-MV) and MG-labeled nonspecific immunoglobulin G (MG-IgG) were transported to the growth cone and filopodial area (Fig. 1, D and E), and MG labeling of anti–myosin-V (*15*) had no detectable effect on antibody binding to purified myosin-V in vitro (*16*).

To show that CALI could affect myo-

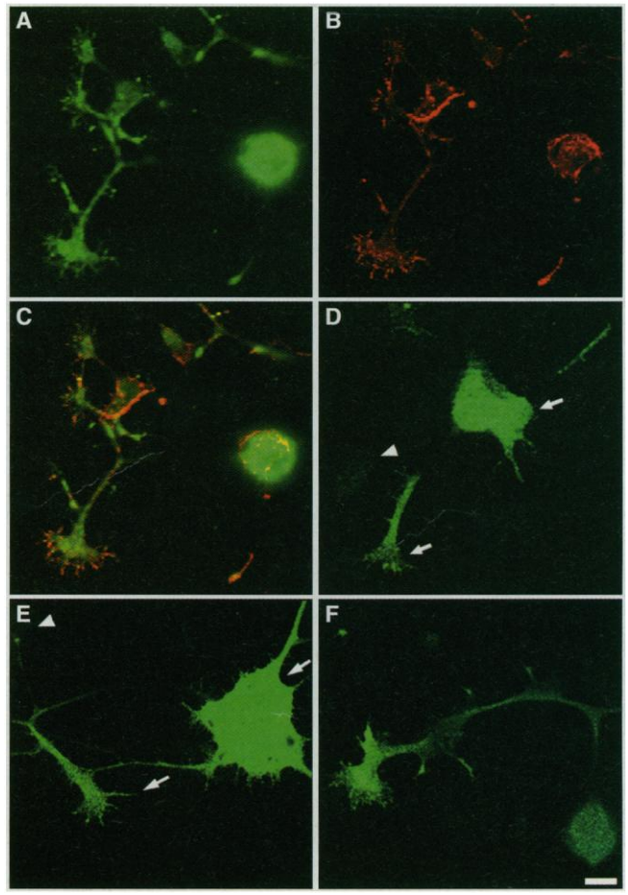

Fig. 1. Localization by confocal microscopy of myosin-V and myosin-Iβ in cultured chick DRG neurons. Indirect immunofluorescence was used to detect the localization of myosin-V, F-actin, and myosin-Iβ in DRG neurons (*10*). (**A**) Myosin-V staining pattern (green) obtained with a polyclonal antibody to myosin-V tail domain. (**B**) F-actin staining pattern (red) in the same growth cones and cell body obtained with rhodamine-phalloidin. (**C**) Superimposed image of (A) and (B) showing localization overlap of myosin-V and F-actin in filopodia (yellow). (**D** and **E**) Anti–myosin-V and nonspecific IgG staining pattern after microinjection. Cell body and growth cone of injected cells were stained (arrows), whereas noninjected cells were not stained (arrowheads). (**F**) Myosin-Iβ staining pattern obtained with anti–myosin-Iβ (M2). Microinjection of the antibody showed a similar staining pattern. Scale bar, 10 μm.

F.-S. Wang and D. G. Jay, Department of Molecular and Cellular Biology, Harvard University, 16 Divinity Avenue, Cambridge, MA 02138, USA.
J. S. Wolenski, R. E. Cheney, M. S. Mooseker, Department of Biology, Yale University, New Haven, CT 06520, USA.

*Present address: Department of Physiology, University of North Carolina, Chapel Hill, NC 27599, USA.
†To whom correspondence should be addressed. E-mail: jay@biosun.harvard.edu

sin-V function, we assessed the motor and adenosine triphosphatase (ATPase) activities of myosin-V in vitro after incubation with MG–anti-MV and exposure to laser irradiation. CALI of purified myosin-V absorbed onto the nitrocellulose-coated surface of motility chambers completely inhibited the ability of this motor to translocate actin filaments (Table 1) (*16*). In contrast, myosin-V in the unirradiated areas of the same motility chambers translocated actin filaments (Table 1). Irradiated myosin-V in the presence of MG–anti-MV was able to bind actin without adenosine triphosphate (ATP), but upon the addition of ATP, actin filaments gradually detached from the immobilized motors and exhibited Brownian motion. The loss of motor activity probably resulted from the damage produced by MG–anti-MV bound to the immobilized myosin-V. CALI of myosin-V in solution had no effect on its Mg^{2+}-ATPase activity (*17*). This result is consistent with rotary shadowed images of myosin-V showing that the distance between the antibody-binding site (or sites) on the tail and the ATPase domain in the myosin-V head (>100 Å) is beyond the range of photochemical damage of CALI (half-maximal radius ~15 Å) (*8*, *10*). Thus, CALI selectively inactivates functional domains that are far apart in a protein's structure.

Chick DRG neurons were microinjected with MG–anti-MV, and selected areas of the growth cone were laser-irradiated to inactivate myosin-V (*18*). Neurons were then observed with time-lapse video microscopy for changes in growth cone motility. Micro-CALI of myosin-V caused marked retraction of filopodia inside the laser irradiation area, whereas filopodia of the same growth cone outside of the irradiated area were not affected (Fig. 2, A and B). Retraction of filopodia began at 1.5 ± 0.6 min (mean ± SEM; n = 13) after the initiation of laser irradiation. Quantitative analysis of filopodial length showed that during the 5-min laser irradiation period, significant filopodial retraction occurred inside the laser-irradiated area only and continued for the duration of the 10-min post-irradiation observation period (Table 2). In contrast, laser irradiation of neurons inject-

Table 1. CALI of purified myosin-V blocks the ability of myosin-V to translocate actin filaments in vitro. Actin filament sliding speeds of myosin-V ± SEM in the presence of either MG-IgG or MG–anti-MV with or without laser irradiation (*16*). The number of data points is given in parentheses.

Condition	Average velocity (nm/s)
Myosin-V	286 ± 10.4 (50)
Myosin-V + MG-IgG (outside laser area)	160 ± 7.4 (20)
Myosin-V + MG-IgG (inside laser area)	206 ± 12.2 (20)
Myosin-V + MG–anti-MV (outside laser area)	195 ± 9.1 (33)
Myosin-V + MG–anti-MV (inside laser area)	No observed motility

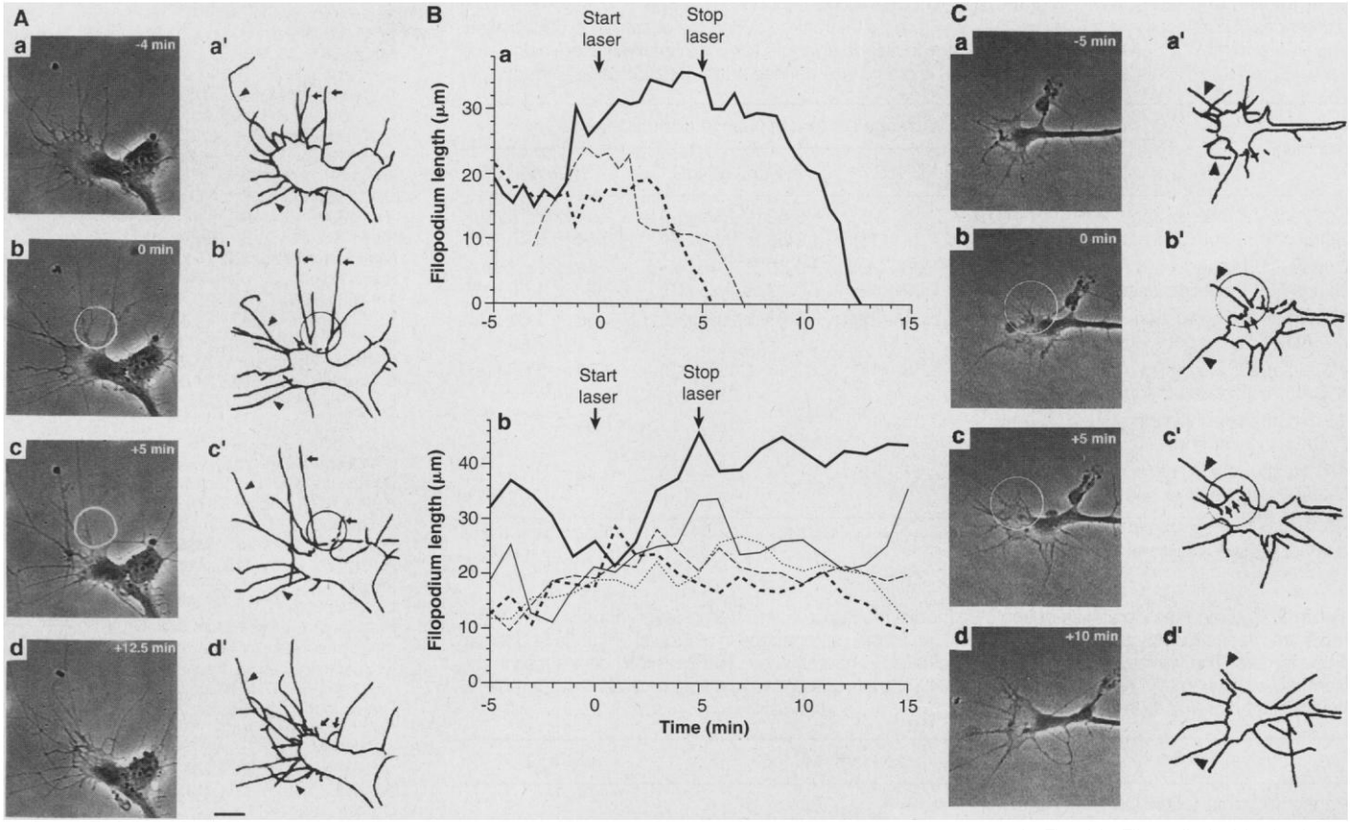

Fig. 2. Micro-CALI of myosin-V in vivo. In all experiments, the growth cone of an injected neuron was observed for 5 min (−5 to 0 min), irradiated for 5 min (0 to 5 min), and further monitored for 10 min (+5 to +15 min) (*18*). (**A**) Series of phase images (a to d) and camera lucida drawings (a′ to d′) of a growth cone injected with MG–anti-MV. (a and a′) A growth cone before laser irradiation; (b and b′) beginning of growth cone laser irradiation (within circle); (c and c′) end of partial growth cone laser irradiation; (d and d′) 12.5 min after the initiation of laser irradiation. The filopodia inside the laser area (arrows) retracted, whereas those outside (arrowheads) did not. (**B**) Filopodial length changes of the growth cone shown in Fig. 2A. Filopodia inside the laser-irradiation area retracted after irradiation (a), whereas filopodia outside the laser-irradiated area did not show retraction (b). (**C**) Series of phase images (a to d) and camera lucida drawings (a′ to d′) of a growth cone injected with MG–anti-MIβ. (a and a′) A growth cone before laser irradiation; (b and b′) beginning of laser irradiation (within circle); (c and c′) end of laser irradiation; (d and d′) 10 min after the initiation of laser irradiation. Filopodia inside the laser area did not retract (arrowheads), whereas the leading edge of lamellipodia inside the laser area expanded (parallel arrows). Scale bar, 10 μm.

ed with MG-IgG did not cause significant change in filopodial length and filopodial dynamics (Table 2).

The retraction of filopodia was likely due to the specific inhibition of myosin-V function rather than to the inactivation of actin, or actin-associated proteins, or a nonspecific response to laser irradiation, because micro-CALI of talin and vinculin resulted in distinct morphological alterations but not significant filopodial retraction (*19*). Moreover, micro-CALI of myosin-Iβ with MG-labeled anti–myosin-Iβ (M2) (MG–anti-MIβ) (*20*) induced lamellipodial expansion inside the laser-irradiated area, but did not cause a significant filopodial retraction (Fig. 2C and Table 2). Myosin-Iβ is a single-headed unconventional myosin concentrated in the growth cone body (Fig. 1F) and actin-rich peripheral structures (*7*, *20*). The increase of lamellipodial size in the irradiated area was observed in 8 out of 15 growth cones during the 5-min laser-irradiation period (Fig. 2C) [27.4 ± 9.8% (mean ± SEM; n = 15) versus 2.1 ± 4.7% (n = 13) outside the laser-irradiated region, $P < 0.05$]. In contrast, no significant lamellipodial expansion was detected in 15 neurons injected with MG-IgG or 18 neurons injected with MG–anti-MV. That CALI of a second myosin isoform has different effects on actin-based motility argues strongly against nonspecific effects of CALI on the cytoskeleton.

The observed net filopodial retraction in response to micro-CALI of myosin-V resulted from an increase in the relative amount of time that filopodia spent in retraction and a significant decrease in the rate of filopodial extension (Table 3). In contrast, micro-CALI of myosin-V did not alter the rate of filopodial retraction. Thus, myosin-V functions in filopodial extension, and filopodial extension and retraction are likely to be independently regulated. One explanation for the filopodial retraction is that CALI resulted in the inhibition of myosin-V motor function. Alternatively, the retraction could be due to the disruption of the interactions between myosin-V tail domain and the membrane because myosin-V is thought to associate with membranous components through its tail domain (*7*, *8*).

We have presented direct evidence of a role for a particular myosin in growth cone filopodial dynamics. The acute nature of the inactivation caused by CALI allows determination of a motor's cellular function with a resolution unattainable in temperature-shift experiments with conditional myosin mutants (*21*). The assessment of a myosin motor's function after CALI may differ from that in experiments with myosin mutants, such as the *dilute* mouse or Myo2 in yeast (*22*), in which the loss of myosin is systemic and chronic and cells may establish compensatory strategies that use functionally redundant myosins as substitutes for the deleted protein.

Table 2. Statistical analysis of filopodial dynamics after micro-CALI. The number of filopodia (n) that were tracked and measured during the 20-min observation period is indicated in parentheses. The differences in n reflect the fact that not all filopodia could be tracked during the observation period. Data shown are means ± SEM. Average net changes in filopodial length for 5-min intervals were calculated from −5 min to +15 min after laser irradiation. Time zero was defined at the initiation of laser irradiation.

Condition	Average net length change (μm) ± SE (n)		
	MG–anti-MV IgG	MG–anti-MI IgG	MG-IgG
Before CALI, in laser spot	−0.67 ± 2.13 (20)	−0.62 ± 1.39 (14)	−1.61 ± 1.15 (18)
Before CALI, outside laser spot	+1.20 ± 1.24 (18)	+0.63 ± 2.59 (9)	+0.74 ± 3.46 (12)
During CALI, in laser spot	−4.82 ± 1.98* (20)	+0.50 ± 1.46 (15)	+1.71 ± 1.61 (20)
During CALI, outside laser spot	+0.79 ± 1.09 (12)	−0.12 ± 2.28 (10)	−2.97 ± 1.90 (20)
10 min after the initiation of CALI, in laser spot	−9.14 ± 2.31† (20)	+0.83 ± 2.65 (13)	+1.62 ± 1.61 (19)
10 min after the initiation of CALI, outside laser spot	−0.35 ± 1.58 (12)	+0.11 ± 1.71 (9)	+2.62 ± 2.67 (12)
15 min after the initiation of CALI, in laser spot	−16.74 ± 3.55‡ (12)	–	+1.68 ± 1.78 (19)
15 min after the initiation of CALI, outside laser spot	+1.03 ± 2.57 (12)	–	+0.75 ± 2.73 (12)

*$P < 0.05$, †$P < 0.02$, and ‡$P < 0.002$ by analysis of Student's unpaired t tests. The differences among other numbers are not statistically significant ($P > 0.05$).

Table 3. Rate and temporal distribution of filopodial movements after the initiation of micro-CALI. The rates are means (μm/s) ± SEM and were obtained from net changes in filopodial length in sequential video frames. The number of data points is indicated in parentheses. The observed differences in the filopodial extension and retraction rate in chick DRG neurons on laminin substrate are comparable to that of Buettner *et al*. (*23*).

	MG–anti-MV IgG	MG-IgG
Rate of filopodial extension		
In laser spot	0.045 ± 0.011* (42)	0.118 ± 0.024 (32)
Outside laser spot	0.114 ± 0.016 (69)	0.096 ± 0.013 (61)
Rate of filopodial retraction		
In laser spot	0.069 ± 0.009 (63)	0.065 ± 0.018 (42)
Outside laser spot	0.079 ± 0.008 (125)	0.077 ± 0.009 (112)
Percentage of time spent in retraction		
In laser spot	75.7 ± 5.3† (10)	55.0 ± 4.9 (8)
Outside laser spot	50.0 ± 3.2 (8)	50.0 ± 4.2 (8)

*$P < 0.05$, †$P < 0.001$ by Student's unpaired t test. The differences between other rates are not statistically significant.

REFERENCES AND NOTES

1. C. S. Goodman and C. J. Shatz, *Cell* **72**/*Neuron* **10** (suppl.), 77 (1993); S. M. Strittmatter and M. C. Fishman, *BioEssays* **13**, 127 (1991).
2. R. W. Davenport, P. Dou, V. Rehder, S. B. Kater, *Nature* **361**, 721 (1993); T. Mitchison and M. Kirschner, *Neuron* **1**, 761 (1988); J. Q. Zheng, M. Felder, J. A. Connor, M. M. Poo, *Nature* **368**, 140 (1994).
3. C.-H. Lin and P. Forscher, *Neuron* **14**, 763 (1995).
4. A. K. Lewis and P. C. Bridgman, *J. Cell Biol.* **119**, 1219 (1992); J. V. Small, M. Herzog, K. Anderson, *ibid.* **129**, 1275 (1995).
5. C. S. Peskin, G. M. Odell, G. F. Oster, *Biophys. J.* **65**, 316 (1993).
6. M. P. Sheetz, D. B. Wayne, A. L. Pearlman, *Cell Motil. Cytoskeleton* **22**, 160 (1992); C. H. Lin, E. M. Espreafico, M. S. Mooskeker, P. Forscher, *Neuron* **16**, 769 (1996).
7. W. M. Bement, T. Hasson, J. A. Wirth, R. E. Cheney, M. S. Mooseker, *Proc. Natl. Acad. Sci. U.S.A.* **91**, 6549 (1994); *ibid.*, p. 11767; M. S. Mooseker and R. E. Cheney, *Annu. Rev. Cell Dev. Biol.* **11**, 633 (1995); L. P. Cramer and T. J. Mitchison, *J. Cell Biol.* **131**, 179 (1995).
8. R. E. Cheney *et al.*, *Cell* **75**, 13 (1993).
9. E. M. Espreafico *et al.*, *J. Cell Biol.* **119**, 1541 (1992).
10. D. G. Jay and H. Keshishian, *Nature* **348**, 548 (1990); K. G. Linden, J. C. Liao, D. G. Jay, *Biophys. J.* **61**, 956 (1992); J. C. Liao, L. Berg, D. G. Jay, *Photochem. Photobiol.* **62**, 923 (1995); J. C. Liao, J. Roider, D. G. Jay, *Proc. Natl. Acad. Sci. U.S.A.* **91**, 2659 (1994).
11. H. Y. Chang, K. Takei, A. M. Sydor, T. Born, F. Rusnak, D. G. Jay, *Nature* **376**, 686 (1995); P. Diamond *et al.*, *Neuron* **11**, 409 (1993).
12. D. Schmucker, A. Su, A. Beermann, H. Jackle, D. G. Jay, *Proc. Natl. Acad. Sci. U.S.A.* **91**, 2664 (1994); R. Schroeder, D. G. Jay, D. Tautz, *Dev. Genes Funct.*, in press.
13. J. S. Wolenski, R. E. Cheney, P. Forscher, M. S. Mooseker, *J. Exp. Zool.* **267**, 33 (1993); J. S. Wolenski, R. E. Cheney, M. S. Mooseker, P. Forscher, *J. Cell Sci.* **108**, 1489 (1995).
14. Chick DRGs from E10 to E12 embryos (Spafas, Preston, CT) were obtained as described [D. Bray, in *Culturing Nerve Cells*, G. Banker and K. Goslin, Eds. (MIT Press, Cambridge, MA, 1991), pp. 119–135]. The neurons were then plated onto cover slips coated with poly-L-lysine (1 mg/ml) and laminin (0.1 mg/ml; Sigma). After a 3- to 5-hour incubation at 37°C, cells were fixed, permeabilized, and incubated with affinity-purified polyclonal antibody to myosin-V (2 μg/ml) and monoclonal antibody to myosin-Iβ (M2) (5 μg/ml) at 4°C overnight. Neurons were then

probed with fluorescein-conjugated secondary antibodies (1:100 dilution; Jackson ImmunoResearch Labs) and rhodamine-phalloidin (0.66 μM; Molecular Probes). Immunostaining after microinjection of MG-labeled antibodies (1 mg/ml) into neurons with or without fluorescent dextran marker was done by directly incubating with fluorescent secondary antibody. Images were taken with a Zeiss LSM 410 confocal microscope equipped with a 63× plan-Apochromat [numerical aperture (NA) = 1.4] oil-immersion lens.

15. D. G. Jay, *Proc. Natl. Acad. Sci. U.S.A.* **85**, 5454 (1988). All antibodies were labeled with MG to the same ratios (6 to 9 dyes per IgG molecule).
16. Sliding actin filament assay was done essentially as described (*13*). Briefly, myosin-V (25 μg/ml) was perfused into motility chambers and allowed to absorb onto the nitrocellulose cover slips for 10 min. After rinses with blocking buffer to remove unbound myosins, MG-labeled antibodies (47.5 μg/ml; molar ratio myosin-V:IgG = 1:7) were added to the chamber and incubated for 30 min. After the removal of unbound antibodies, half of the motility chambers were marked with ink and subjected to laser irradiation for 5 min. After the addition and examination of actin filaments (rhodamine-phalloidin F-actin; 12 nM) in the absence of ATP, sliding was initiated by the addition of motility buffer containing 2 mM ATP. The density of bound actin filaments was indistinguishable between laser-irradiated and unirradiated areas before the initiation of motility. After the addition of ATP, most of the filaments inside the irradiated area were released intact, although a few exhibited Brownian motion and detached gradually. Motility was recorded with a Nikon Diaphot 300 microscope equipped with epifluorescence optics (Plan Apo 100× NA 1.4 oil-immersion objective) and a Dage-MTI SIT camera. Time-lapse images were digitized with MetaMorph image acquisition software (Universal Images, PA) and then transferred to an optical laser disc recorder. Motility assays were done at 24° ± 1°C. A yttrium-aluminum-garnet–Nd (YAG-Nd)–pumped dye laser (models GCR11 and PDL2, Spectra Physics) was used to generate a 620-nm light at an energy output of 18 mJ per pulse (2-mm-diameter laser spot).
17. Chick brain myosin-V was purified and Mg^{2+}ATPase assays were done as described (*8*). Samples contained a final concentration of 4.5 μg/ml myosin-V, 860 μg/ml F-actin, and 430 μg/ml calmodulin. Aliquots were incubated for 0 or 7 min at 37°C in ATPase buffer. For CALI assays, myosin-V was incubated with either MG–anti-MV or MG-IgG (molar ratio myosin-V:IgG = 1:7) for 30 min and then laser-irradiated for 5 min before assessment with ATPase assay (*16*). Laser irradiation of purified myosin-V in solution had no effect on the actin-activated Mg^{2+}-ATPase activity of myosin-V (24.70 ± 0.10 versus 27.15 ± 0.75 without irradiation). Further, CALI did not inhibit myosin-V ATPase activity in the presence of MG–anti-MV (16.80 ± 2.00 versus 16.95 ± 2.95 without irradiation) or MG-IgG (17.95 ± 2.95 versus 18.40 ± 1.00 without irradiation). Results are the averages ± SEM from three independent assays. ATPase activities are given in ATP molecules per myosin-V head per second.
18. Chick DRG cultures were maintained at 37°C on the microscope stage with a stage incubator. MG-labeled antibodies mixed with fluorescein-dextran (3 mg/ml; Molecular Probes) were microinjected into neurons. After a 30- to 60-min incubation, healthy neurons were selected for micro-CALI experiments (*11*). A selected area of the growth cone was observed for 5 min, subjected to laser irradiation for 5 min, and followed for an additional 10-min examination with a Zeiss Axiovert 10 microscope with phase-contrast optics. Time-lapse images (one frame every 15 s) and image enhancements were facilitated by custom-written software and recorded on an optical laser disc recorder (*11*). The laser beam for micro-CALI was generated with a nitrogen-pumped dye laser (model VSL-337, Laser Science) at an energy output of 30 μJ per pulse (10-μm-diameter laser spot).
19. A. M. Sydor, A. Su, F.-S. Wang, A. Xu, D. G. Jay, *J. Cell Biol.*, in press.
20. B. Barylko, M. C. Wagner, O. Reizes, J. P. Albanesi, *Proc. Natl. Acad. Sci. U.S.A.* **89**, 490 (1992); M. C. Wagner, B. Barylko, J. P. Albanesi, *J. Cell Biol.* **119**, 163 (1992).
21. M. L. Springer, B. Patterson, J. A. Spudich, *Development* **120**, 2651 (1994).
22. B. Govindan, R. Bowser, P. Novick, *J. Cell Biol.* **128**, 1055 (1995); G. Jung and J. Hammer, *ibid.* **110**, 1955 (1990); J. A. Mercer, P. K. Seperack, M. C. Strobel, N. G. Copeland, N. A. Jenkins, *Nature* **349**, 709 (1991); K. Novak and M. Titus, *Mol. Biol. Cell* **3**, 3a (1992); V. R. Simon, T. C. Swayne, L. A. Pon, *J. Cell Biol.* **130**, 345 (1995); M. A. Titus, D. Wessels, J. A. Spudich, D. Soll, *Mol. Biol. Cell* **4**, 233 (1993).
23. H. M. Buettner, R. N. Pittman, J. K. Ivins, *Dev. Biol.* **163**, 407 (1994).
24. We thank A. Xu for technical assistance and J. P. Albanesi (University of Texas Southwestern Medical Center, Dallas) for providing monoclonal antibodies to myosin-Iβ (M2 and M3). Supported in part by National Institutes of Health (NIH) grants NS-29007 and NS-34699 (to D.G.J.) and DK-25387 (to M.S.M.), the Lucille P. Markey Charitable Trust and Klingenstein fellowship (to D.G.J.), and the Pew Charitable Trust (to J.S.W.). F.-S.W. acknowledges receipt of a postdoctoral fellowship from the NIH.

15 January 1996; accepted 20 May 1996

PTH/PTHrP Receptor in Early Development and Indian Hedgehog–Regulated Bone Growth

Beate Lanske, Andrew C. Karaplis, Kaechong Lee, Arne Luz, Andrea Vortkamp, Alison Pirro, Marcel Karperien, Libert H. K. Defize, Chrystal Ho, Richard C. Mulligan, Abdul-Badi Abou-Samra, Harald Jüppner, Gino V. Segre, Henry M. Kronenberg*

The PTH/PTHrP receptor binds to two ligands with distinct functions: the calcium-regulating hormone, parathyroid hormone (PTH), and the paracrine factor, PTH-related protein (PTHrP). Each ligand, in turn, is likely to activate more than one receptor. The functions of the PTH/PTHrP receptor were investigated by deletion of the murine gene by homologous recombination. Most PTH/PTHrP receptor (−/−) mutant mice died in mid-gestation, a phenotype not observed in PTHrP (−/−) mice, perhaps because of the effects of maternal PTHrP. Mice that survived exhibited accelerated differentiation of chondrocytes in bone, and their bones, grown in explant culture, were resistant to the effects of PTHrP and Sonic hedgehog. These results suggest that the PTH/PTHrP receptor mediates the effects of Indian Hedgehog and PTHrP on chondrocyte differentiation.

The PTH/PTHrP receptor responds to two ligands, PTH and PTHrP. PTH is synthesized by the parathyroid glands and acts on kidney and bone to regulate calcium homeostasis (*1*). PTHrP, in contrast, is synthesized in multiple tissues with specific spatial and temporal profiles and has largely paracrine functions (*2*).

Complementary DNA encoding the PTH/PTHrP receptor was cloned from bone and kidney cells. The receptor binds and responds equally to NH_2-terminal fragments of PTH and PTHrP (*3*, *4*). The PTH/PTHrP receptor mRNA is expressed in the PTH target organs, kidney and bone (*5*, *6*), as well as in organs in which PTHrP is expressed, such as extraembryonic membranes and growth plates of bone (*7*, *8*). Physiologic studies suggest that other receptors for PTH and PTHrP exist (*9*–*11*), one of which has been cloned (*12*).

At implantation, the murine PTH/PTHrP receptor is expressed in parietal endoderm immediately adjacent to PTHrP-expressing trophoblastic cells (*7*, *13*). Trophoblastic PTHrP induces the differentiation of the parietal endoderm and the subsequent synthesis of components of Reichert's membrane in vitro (*13*). Nevertheless, mice homozygous for a targeted deletion of PTHrP are normal early in development (*14*) and later manifest only abnormalities in endochondral bone development, and then die at birth.

Chondrocytes in the growth regions of bones of PTHrP (−/−) mice undergo fewer rounds of proliferation than in normal mice and differentiate prematurely into hypertrophic chondrocytes (*14*, *15*). In contrast, bone explants exposed to PTHrP NH_2-terminal fragment have delayed differentiation of hypertrophic chondrocytes (*16*).

B. Lanske, K. Lee, A. Pirro, A.-B. Abou-Samra, H. Jüppner, G. V. Segre, H. M. Kronenberg, Endocrine Unit, Massachusetts General Hospital and Harvard Medical School, Boston, MA 02114, USA.
A. C. Karaplis, Department of Medicine, Sir Mortimer B. Davis–Jewish General Hospital, McGill University, Montreal, Quebec H3T 1E2, Canada.
A. Luz, Institute of Pathology, GSF München, D 85758 Neuherberg, Germany.
A. Vortkamp, Department of Genetics, Harvard Medical School, Boston, MA 02115, USA.
M. Karperien and L. H. K. Defize, Hubrecht Laboratorium, Netherlands Institute for Developmental Biology, 3584 CT Utrecht, The Netherlands.
C. Ho, Department of Genetics and Howard Hughes Medical Institute, Harvard Medical School, Boston, MA 02115, USA.
R. C. Mulligan, Whitehead Institute for Biomedical Research, Cambridge, MA 02142, and Massachusetts Institute of Technology, Cambridge, MA 02139, USA.
*To whom correspondence should be addressed.